On the Quality of the Nimbus 7 LIMS Version 6 Water Vapor Profiles and Distributions

E. E. Remsberg[1], M. Natarajan[1], G. S. Lingenfelser[2]

R. E. Thompson[3], B. T. Marshall[3], and L. L. Gordley[3]

[1]NASA Langley Research Center

21 Langley Blvd., Mail Stop 401B

Hampton, VA 23681 USA

Ellis.E.Remsberg@nasa.gov

[2]SSAI

1 Enterprise Parkway

Hampton, VA 23661 USA

[3]GATS, Inc.

11864 Canon Blvd., Suite 101

Newport News, VA 23606 USA

June 2009

Abstract

This report describes the quality of the Nimbus 7 Limb Infrared Monitor of the Stratosphere (LIMS) water vapor (H_2O) profiles of 1978/79 that were processed with a Version 6 (V6) algorithm and archived in 2002. The V6 profiles incorporate a better knowledge of the instrument attitude for the LIMS measurements along its orbits, leading to improvements for its temperature profiles and for the registration of its water vapor radiances with pressure. As a result, the LIMS V6 zonal-mean distributions of H_2O exhibit better hemispheric symmetry than was the case from the original Version 5 (V5) dataset that was archived in 1982. Estimates of the precision and accuracy of the V6 H_2O profiles are developed and provided. Individual profiles have a precision of order 5% and an estimated accuracy of about 19% at 3 hPa, 14% at 10 hPa, and 26% at 50 hPa. Profile segments within about 2 km of the tropopause are often affected by emissions from clouds that appear in the finite field-of-view of the detector for the LIMS H_2O channel. Zonally-averaged distributions of the LIMS V6 H_2O are compared with those from the more recent Microwave Limb Sounder (MLS) satellite experiment for November, February, and May of 2004/2005. The patterns and values of their respective distributions are similar in many respects. Effects of a strengthened Brewer-Dobson circulation are indicated in the MLS distributions of the recent decade versus those of LIMS from 1978/79. A tropical tape recorder signal is present in the 7-month time series of LIMS V6 H_2O with lowest values in February 1979, and the estimated, annually-averaged "entry-level" H_2O is 3.5 to 3.8 ppmv. It is judged that this historic LIMS water vapor dataset is of good quality for studies of the near global-scale chemistry and transport for pressure levels from 3 hPa to about 70 to 100 hPa.

1. Background

The Nimbus 7 Limb Infrared Monitor of the Stratosphere (LIMS) experiment operated successfully from 25 October 1978 through 28 May 1979, the planned lifetime of the onboard cryogen gases used to cool its detectors (Gille and Russell, 1984). LIMS provided daily, near-global distributions of stratospheric H_2O. The LIMS Version 5 (V5) Level 2 profiles and Level 3 zonal Fourier coefficients were archived in 1982 and 1983, respectively, and they have been used for numerous scientific studies. The present report describes the quality of the updated, Version 6 (V6) H_2O dataset, archived in 2002.

As a review, it is noted that the original, LIMS V5 H2O distributions were used to examine issues related to stratospheric chemistry (e.g., LeTexier et al., 1988; Garcia and Solomon, 1994) and transport (e.g., Gray and Pyle, 1986; Butchart and Remsberg, 1986; and Gille et al., 1987). Its H_2O distributions were also used in studies of the stratospheric budget of water vapor, and, in particular, to estimate the H_2O mixing ratio as it enters the tropical stratosphere from below (Jones et al., 1986; Hansen and Robinson, 1989). Their estimated, annually-averaged, "entry-level" values ranged from 2.7 ppmv to 3.3 ppmv. Russell (1987) and Remsberg et al. (1990) provided the monthly distributions of stratospheric H_2O from the LIMS V5 Level 3 (mapped) dataset. Later, Chiou et al. (1993; 1996) compared the LIMS V5 distributions with those from the Stratospheric Aerosol and Gas Experiment (SAGE II) of the Earth Radiation Budget Satellite (ERBS) and from the Stratospheric and Mesospheric Sounder (SAMS) instrument of Nimbus 7. They found general agreement among those three data sets, at least within their combined

error bars. However, the H_2O values from all three experiments were subject to rather large errors, particularly in the lower stratosphere. Their respective meridional gradients of H_2O also differed somewhat with each other and with those obtained from subsequent ER-2 aircraft measurement campaigns.

The precisions and accuracies for the LIMS V5 H_2O profiles were reported in Russell et al. (1984), Remsberg et al. (1984a), and Remsberg and Russell (1987). Their combined errors are no greater than 17% in the middle stratosphere (3 to 30 hPa), due primarily to the effects of profile registration and temperature biases for their retrievals. Their quality is not as good near the stratopause because that is where the radiances approach the detector noise for the H_2O channel. In the upper stratosphere the radiances originate from strong water vapor lines in the LIMS broadband H_2O channel from 6.4 to 7.3-μm. Those lines are nearly saturated and lead to a highly non-linear relation between radiance and retrieved H_2O concentration. Kerridge and Remsberg (1989) reported on the effects of an additional complication for the retrieval of upper stratospheric LIMS H_2O, particularly during daylight. They showed that the retrieved H_2O values at those altitudes were larger for day than for night--a consequence of not accounting for non-local thermodynamic equilibrium (non-LTE) emissions in the daytime H_2O radiances. That additional, non-LTE emission is most significant in the mesosphere, but its residual effects also extend to the profile segments of the upper stratosphere (Mertens et al., 2002).

The LIMS V5 H_2O is also not very accurate in the upper troposphere/lower stratosphere (UT/LS) (Kley et al., 2000). In particular, there are systematic H_2O errors just above the tropical tropopause due to the LIMS V5 temperatures being a bit too warm, to the uncertainties for the interfering effects of the pressure-induced O_2 continuum emission, and to the contaminating emissions from aerosols and clouds that were not accounted for. Furthermore, in the tropics there is a sharp increase of H_2O and temperature just below the tropopause. The instantaneous, finite vertical field-of-view (FOV) width of the LIMS H_2O channel averages across the region of the tropopause and provides H_2O profiles having a vertical resolution of about 4.5 km. Although the deconvolution procedure accounts for the effects of any FOV side lobes in the radiances prior to their retrieval, the spatial smoothing effect of the main FOV lobe is still present.

Section 2 of this report describes the important changes in the LIMS V6 water vapor algorithm and the improvements for its profiles and distributions. Its zonally-averaged, nighttime distribution for mid November is compared qualitatively with the Earth Observing System (EOS Aura) Microwave Limb Sounder (MLS) Version 2.2 (v2.2) H_2O of 2004. Both cross sections exhibit many of the same features. Section 3 gives estimates of the precision and systematic errors for single LIMS V6 H_2O profiles. Section 4 contains qualitative comparisons between LIMS and MLS for February and May. Although their overall distributions are similar, they show significant differences near the tropical hygropause and in the upper stratosphere at high latitudes. Section 5 contains a brief discussion of some initial scientific findings from the LIMS distributions, and Section 6 summarizes the quality of the V6 H_2O dataset.

2. LIMS V6 Water Vapor

2.1. LIMS V6 algorithm for H_2O

A major reason for the update of the overall LIMS algorithm to V6 is the incorporation of more recent spectroscopic line parameters for the retrievals of the LIMS profiles of temperature and each of its species (ozone, water vapor, nitric acid, and nitrogen dioxide), so that they are more compatible with the corresponding profile quantities obtained with the follow-on sensor systems of the Upper Atmosphere Research Satellite (UARS), of EOS Aura, and of the Environmental Satellite (ENVISAT) of the European Space Agency. The V6 forward model for the H_2O and CH_4 radiances in the LIMS channel makes use of HITRAN 1996 line parameters (Rothman et al., 1998), although the parameters for the ν_2 lines of H_2O from 6.4 to 7.3 μm are nearly unchanged from the ones used for the retrieval of the earlier V5 profiles. Effects of overlap for the lines of H_2O and CH_4 are accounted for with an additional, band model emissivity table. The effects of the underlying, interfering radiance from the O_2 continuum are updated based on the empirical model of Thibault et al. (1997). The temperature dependence of that model is significantly different from what was used for O_2 in V5, particularly for the colder temperatures of the lower stratosphere. This change is one reason that the retrieved V6 H_2O profiles of the tropical lower stratosphere are not quite as dry as those of V5.

The Nimbus 7 spacecraft was in a Sun-synchronous orbit, and the LIMS radiometer viewed the atmospheric limb and in a direction 146.5 degrees clockwise from the spacecraft velocity vector (Gille and Russell, 1984). Figure 1 is a projection of the

instantaneous FOVs for the LIMS channels at the atmospheric limb for the tops and bottom of a down/up scan pair, traveling from right to left along the orbit. The angular resolution for the H_2O detector is 1 milliradian, and it subtends a vertical width of 3.6 km for the tangent layer at the horizon. Effectively, it is the geometry of the limb measurement that determines the vertical resolution of its retrieved profiles.

Accuracies for the LIMS H_2O profiles are dominated by the uncertainties in the atmospheric temperature-pressure profiles (or T(p)) and the associated registration of the H_2O radiances with pressure-altitude (Russell et al., 1984). The better determination of spacecraft/instrument orbital attitude for LIMS V6 led to an improved registration for the radiances and more accurate T(p) values. The point spacing for the measured Level 2 profile data is 0.375 km from all the LIMS channels. However, one can see from Figure 1 that the CO_2 channels used to retrieve T(p) have a vertical width that is half that of the water vapor channel. The potential mismatch between the two was overcome by the methods used to condition the radiances for instrument effects and by the interleave retrieval approach, together leading to an effective vertical resolution of 3.7 km for all the radiance profiles (Remsberg et al., 2004). As a result, the V6 H_2O profiles and distributions have a quality and stability that is improved over that from the original V5 algorithm. The retrieved V6 temperatures are closely compatible with the H_2O radiances, such that the effect of any vertical temperature structure is not very noticeable in the retrieved H_2O profiles. A Gaussian smoother with a nearly 1.5 km vertical halfwidth at half maximum was employed for the final retrieval of the H_2O profiles. The V6 profiles

were also output at the more frequent spacing of about 1.6 degrees of latitude along an orbit, rather than the nearly 4 degree separations of the V5 dataset.

First-order corrections for the interfering effects of CH_4 were achieved using the seasonal, zonal mean cross sections of 1994 from the UARS Halogen Occultation Experiment (HALOE) dataset, but extrapolated back to 1979 based on the annually-increasing CH_4 at ground level. Note that we did not elect to use the concurrent CH_4 distributions from the Nimbus 7 Stratosphere and Mesosphere Sounder (SAMS) experiment because they only extended down to about the 20-hPa level (Jones and Pyle, 1984). A similar first-order correction for the interfering emissions from stratospheric aerosols was developed based on the 5.26-μm aerosol extinctions of March/May 1996 from HALOE, but then extrapolated back to 1979 based on the ratio of the SAGE I extinctions at 1 μm for 1979 to the corresponding SAGE II extinctions of 1996. A minor extrapolation was also performed to convert the HALOE extinctions from 5.26 to 6.9 μm. However, the near-background aerosols of the LIMS time period have only a minor effect for the forward radiance model of its H_2O channel. On the other hand, the accounting for CH_4 leads to a reduction of tropical H_2O mixing ratios by 15% between about 40 to 7 hPa. Effects of horizontal temperature gradients along the view path for the tangent-layer have also been accounted for to first order within the V6 algorithm (Remsberg et al., 2004).

The V6 H_2O retrievals are based on a downward, onion-peeling approach, rather than an optimal estimation procedure. Retrievals began where signal-to-noise (S/N) values for the radiances exceed a value of 1.5—in the lower mesosphere. V6 temperatures are

warmer than those of V5 by 1 to 2 K at and above the stratopause, so the useful V6 values of H_2O begin several layers lower than for V5. A constant H_2O value of 6.5 ppmv was used in the LIMS forward radiance model to estimate the effects of water vapor radiance above the altitude of the first retrieved layer. That assumed value is based on observations of H_2O for the lower mesosphere from HALOE and MLS and from ground-based microwave measurements of the 1990s, with a slight downward adjustment for the lower values of CH_4 and their oxidation to H_2O for the 1978/79 period (Remsberg et al., 1984).

2.2 LIMS V6 zonal mean distributions of H_2O

Figure 2(a) is the zonally-averaged distribution of V6 H_2O for 15 November 1978 from its descending (north-to-south or local nighttime) orbital segments. General features that are apparent are: (1) the increase of water vapor from the lower to the upper stratosphere due to the chemical conversion of CH_4 to water vapor with altitude, (2) the increase of water vapor in the lower stratosphere from near the Equator to higher latitudes or from the entry region of dry air to the stratosphere to a region of more well-mixed air, and (3) a region of rapid increase from the "tropical hygropause" to just below the tropopause near 100 hPa, where the water vapor begins to increase rapidly. In addition, many of the low altitude portions of the profiles were cutoff due to a first-order screening for the presence of the interfering emissions from clouds, as evaluated based on the character of the corresponding LIMS ozone profiles that are affected very little by the increasing water vapor of the upper troposphere (Remsberg et al., 2007).

Only a very few (less than 10) middle latitude, correlative water vapor profiles were obtained during 1978/79 for the purpose of validating the LIMS H_2O profiles. Those few comparisons indicate that the LIMS V6 values are higher by 10 to 15% from about 10 to 70 hPa, but within the estimated accuracies of about +/-20% for both the comparison measurements (Russell et al., 1984) and the LIMS V6 data themselves (see also Section 3). Consequently, in this report we are opting to show qualitative comparisons of the zonal mean distributions of LIMS V6 versus those from Aura MLS, which have been validated more extensively. The MLS Version 2.2 H_2O distributions are based on profiles having a vertical resolution in the stratosphere (~3-4 km) that is comparable to that of LIMS V6. Precision of individual MLS stratospheric H_2O profiles is about 5%, and accuracy is of the order of 10% (Lambert et al., 2007).

Figure 2(b) is a plot of MLS V2.2 stratospheric H_2O for 15 November 2004 based on data that were accessed from (http://mls.jpl.nasa.gov/). The period of 2004/2005 of the MLS data was selected for comparison because the distribution of H_2O is affected slightly by the QBO-induced circulations of the lower stratosphere and the winds were in the same easterly QBO phase as was the case for the LIMS period (Fueglistaler and Haynes, 2005). Although MLS H_2O extends to near the mesopause, Figure 2(b) is restricted to the same pressure-altitude domain as that of LIMS in Figure 2(a). MLS data extend from 83S to 83N latitude, whereas the LIMS plot covers only from 64S to 84N. It is noted that there is a vertical oscillation in the MLS v2.2 H_2O distribution near 30 hPa that stretches across most latitudes; that feature is an artifact due to departures from a

linear signal response at that level. The MLS data were smoothed to first order according to the prescription in Lambert et al. (2007), prior to the generation of Figure 2(b).

The patterns of zonally-averaged water vapor agree well in most respects between LIMS and MLS, and their absolute values agree within about 10% in the middle stratosphere. MLS has values at 3 hPa that are slightly larger than those of LIMS, a finding that is consistent with the fact that CH_4 has been increasing in the stratosphere since the LIMS time period. The respective meridional gradients of H_2O are largest in the subtropics of the middle stratosphere, which is characteristic of the net transport of the Brewer/Dobson circulation plus the slow chemical conversion of CH_4 to H_2O with altitude. The altitudes of the tropical hygropause and the magnitudes of the minimum water vapor are also similar for the LIMS and MLS distributions of Figure 2, indicating that the effects of the finite FOV and, in particular, the vertical weightings for the temperature and species are being handled properly in the forward radiance model of LIMS V6. That agreement is also an important indicator of the good accuracy of the LIMS V6 T(p) and of the associated pressure registration of its water vapor radiances. On the other hand, one can clearly see the effects of dehydration in the MLS data at 60S, but not in the LIMS cross section at the same latitude. This difference is most likely an indication of the expanded area and persistence of the cold, wintertime southern polar vortex and its associated polar stratospheric clouds (PSC) during the intervening 26 years (WMO, 2007). We will show LIMS and MLS comparisons for February and May in Section 4, so that one can also judge the level of agreement for the seasonal variations of their water vapor distributions.

As with LIMS V5, no corrections are made for the vibrationally-excited (non-LTE) H_2O emissions, the effects of which are most significant in the mesosphere during daytime but which extend down to the uppermost stratosphere, too (Mertens et al., 2002). Figure 3 shows that the retrieved, zonally-averaged daytime V6 H_2O is larger than that for nighttime by about 0.4 to 0.8 ppmv in the upper stratosphere for November 15. Although there are rather large variations in those differences with latitude, note that there is almost no difference poleward of about 60N (twilight or darkness for both the LIMS ascending and descending orbital segments). The nighttime LIMS H_2O distributions ought to be more accurate because the effect of any non-LTE bias is much smaller in the absence of sunlight. But, the effects of non-LTE emissions on the LIMS V6 H_2O of the upper stratosphere are also complicated by the fixed H_2O value of 6.5 ppmv that was used for both day and night in the LIMS forward model above the first retrieved layer. Thus, the day/night differences of the upper stratosphere are not due solely to the non-LTE effects. Day/night H_2O differences at 10 hPa and through the lower stratosphere are less than about 0.4 ppmv. Thus, if one wants to obtain better detail about the daily variations and the transport of H_2O with longitude, it is considered acceptable to combine the ascending (daytime) and descending (nighttime) LIMS data in that pressure-altitude range.

3. Estimates of Error for Single Profiles

Figure 4 is an estimate of the precision for a V6 H_2O profile, as obtained from sets of about 6 scans along each of the orbital segments between 25S and 35S latitude on 1 February 1979, i.e., for a season when the large-scale, zonal wave activity was small for

the stratosphere. The profile points in Figure 4 are actually based on the minimum standard deviation (SD) values from among all the sets of the separate descending (open diamonds) and then the ascending (solid diamonds) orbital segments. Even though there must be effects of atmospheric variability contained in them, those SD values are no worse than about 4% through much of the stratosphere. The much larger SD values near 100 hPa may be due to not having screened effectively for the emissions from thin cirrus. Single profiles of H_2O also have higher SD values near 1.3 hPa because digitization and detector noise is significant for the measured radiances at and above that level.

Table 1 summarizes our calculations of precision (or random error) based on S/N, as well as the effects of systematic errors for a single H_2O profile. The precision is no worse than about 5% through most of the stratosphere, and it is a slight improvement from that for V5--a consequence of the better vertical sampling for the radiances plus the use of a 5-interleave retrieval procedure for obtaining the final V6 profiles (Remsberg et al., 2004). Our calculated precisions are somewhat larger than the SD values of Figure 4.

Estimates of the systematic errors in Table 1 due to radiometric bias, H_2O line parameter uncertainties (8%), the main IFOV lobe, and the approximations for the forward model were adopted from the simulation studies in Russell et al. (1984). The H_2O profiles have a bias of order 10 to 15% due to estimates of the V6 temperature biases from Remsberg et al. (2004, their Table 2, row g), which are less than ±1.6 K as shown in parentheses in Table 1. Furthermore, there is no evidence that the estimated V6 T(p) biases of Table 1 are all of the same sign. That finding is based on the V5 versus rocketsonde/radiosonde

T(p) comparisons in Remsberg et al. (1984b), followed by the zonal mean, V6 minus V5 differences for T(p) in Remsberg et al. (2007, their Figure 3). Uncertainties for the O_2 continuum model are of order 10%, although the effect of that model is only important for the retrieved H_2O from about 50 to 100 hPa. The root-sum-squares (RSS) of the bias errors that were evaluated are given in the bottom row of Table 1 and are of the order of 19% in the upper stratosphere, 15% in the middle stratosphere, and 26% in the lower stratosphere. Primary components of that total error are from the uncertainties of the main IFOV lobe and from the estimated temperature biases.

There are other sources of bias error that have not been fully characterized. For example, errors in the spatial side lobes of the IFOV function have not been verified, but their effects appear to be small based on the quality of the V6 H_2O distributions. Small uncertainties are present from the interfering aerosol emission of the lower stratosphere. The distribution of that emission varies with altitude and latitude, and it is representative of the near background aerosol layer of 1978/79. It is also noted that the same monthly and zonally-averaged distribution of aerosol emission was used for making a correction in the forward model for all months of the LIMS dataset. Biases for the interfering CH_4 have their largest effect in the middle to lower stratosphere at tropical latitudes, but they lead to errors in H_2O that are no greater than a few percent. There are also small biases in the retrieved H_2O values at 1.3 to about 2.0 hPa as a result of assuming the constant mixing ratio of 6.5 ppmv for the forward model above the top retrieved layer. Some sources of bias error (such as that from temperature) also vary slightly according to the atmospheric state. In general, the RSS values of Table 1 are considered as worse case

scenario estimates of the true total bias error for a single profile. Finally, the major stratospheric components of the aggregate (~10%) bias error profile for the comparison MLS H_2O data are from pointing uncertainties, forward model assumptions, and the optimal estimation formulation for its retrieval (Lambert et al., 2007).

4. LIMS/MLS Water Vapor Comparisons for February and May

Figure 5(a,b) is a comparison of the zonally-averaged H_2O distributions for 15 February from LIMS in 1979 versus that from MLS in 2005. The agreement between the two is similar to that of November (Figure 2), except for the region of the hygropause which is nearer to the tropopause in February than in November. Specifically, the tropical minimum for 15 February is near 50 hPa to 70 hPa (~20 to 18 km) from LIMS but is near 80 hPa to 100 hPa (~17.5 to 16 km) from MLS. Few of the tropical LIMS profiles actually extend to 100 hPa, and it is very likely that even those few contain effects of residual emissions from thin cirrus. Limb infrared measurements are very sensitive to emissions from clouds, while the microwave measurements are much less so. Further, when the finite FOV measurements of LIMS are nearing the tropopause, the associated retrieved H_2O will have a high bias even for clear skies because of the sharp increase in the water vapor of the upper troposphere. Therefore, one should be cautious about interpreting the LIMS H_2O within about 2 km of the tropopause, or when lower than about 18 km in the tropics to about 13 km at high latitudes.

In the uppermost stratosphere and at high latitudes of the winter hemisphere the MLS H_2O is greater than that of LIMS V6 by 0.5 to 1.0 ppmv, partly a result of the slow increase of atmospheric CH_4 from 1978/79 to 2004/05 and its conversion to H_2O in the upper stratosphere. The maximum values from the MLS data also support our choice of a constant value of 6.5 ppmv for the LIMS H_2O above the first retrieved layer in the lower mesosphere for the LIMS forward model.

There are indications in the February MLS data of effects of descending air from near the stratopause to the middle stratosphere by its elevated values of H_2O in the NH polar vortex. Conversely, the largest polar H_2O from LIMS is centered near 30 hPa, and the temperatures are too warm in mid February for the occurrence of emissions from PSC. It is noted that the profile segments that were obviously contaminated by PSC earlier in the winter were screened out of the individual LIMS profiles, although residual effects may still be present for those periods. A listing of those occurrences is available in a separate file that is part of the archived LIMS dataset. An important difference for the LIMS versus the MLS retrieval of water vapor is the high sensitivity of the LIMS radiances to the temperature along its line-of-sight emissivity mass path. If there are slight errors in the horizontal (or vertical) temperature gradients, there will also be biases in the retrieved LIMS water vapor (see Table 1). Such biases are a distinct possibility at the edges of the polar vortex and during the sudden stratospheric warming (SSW) periods of January and February 1979. It is presumed that errors in those gradients are the main cause of the apparent excess of polar H_2O from LIMS, spanning from 8 to 80 hPa in mid February.

Figure 6(a,b) shows the LIMS/MLS comparisons for 16 May, and again the distributions are similar in most respects. However, Figure 6a shows that there is an upward and poleward extension of relatively low values of LIMS water vapor (<5.0 ppmv) at about 50S, 3 hPa for May, when there ought to be a slow descent of air from the lower mesosphere with higher H_2O values. The MLS plot of Figure 6b does not show a similar relative minimum. The region of 50S, 3 hPa is very near to the edge of the polar vortex, according to the enhanced meridional gradients of scaled potential vorticity (sPV) and as indicated in the equivalent latitude versus potential temperature (or EqL/θ) plots of the daily MLS water vapor for May (not shown, but viewable at the MLS Website).

In the northern hemisphere there is only a hint of a relative minimum at 50N, 3 hPa in the LIMS plot of Figure 2a for November, when the polar vortex has a similar seasonal configuration. The corresponding MLS plot of Figure 2b shows an H_2O distribution that is very much like that of LIMS. The good agreement between LIMS and MLS in November, but not in May, is explained as follows. The descending orbital segments of LIMS near 50S for May were obtained when the Nimbus 7 satellite was viewing from above the South Pole and the LIMS tangent view path was parallel to the meridional temperature gradient (Remsberg et al., 1986). But because the true temperature field poleward of 64S was not known, the T(p) values at 64S were merely extrapolated poleward for the LIMS emissivity mass path algorithm. Those extrapolated temperatures are too warm and not representative of the southern polar vortex region in May. Such a warm bias means that less of the total radiance in the water vapor channel is attributed to water vapor in the forward model, leading to the relative minimum in LIMS H_2O that was retrieved. The corresponding zonal mean of the ascending LIMS H_2O does not have a

similar relative minimum at 50S, 3 hPa, because the LIMS viewing direction for those orbital segments was more nearly along a line of latitude, and thus the temperature along its view path was known. For the northern hemisphere the LIMS temperatures were retrieved to 84N, and its orbital viewing geometry was also more nearly perpendicular to the temperature gradient. As a result, the LIMS temperatures are likely more accurate in the polar vortex region for the corresponding northern season (c.f., Figure 2a for November).

5. Initial Scientific Findings from LIMS V6 Water Vapor

The Stratospheric Processes and their Role in Climate (SPARC) Project Office has initiated a Re-assessment of the Water Vapor in the Upper Troposphere and Lower Stratosphere (UT/LS) study that is intended to be an update of Kley et al. (2000). The LIMS V6 dataset can be used to extend the historical record of the changes in UT/LS water vapor from the 1978/79 period (see also Rosenlof et al. (2001)). As an example, the LIMS/MLS comparison plots of Figures 2, 5, and 6 show the effects of the classic Brewer/Dobson (BD) circulation in their respective zonal-mean water vapor cross sections, at least for the middle and upper stratosphere.

The isolines of low water vapor mixing ratio above the tropopause are sloping toward higher pressures from low to high latitudes, in accord with a net meridional transport of air along isentropic surfaces. It also appears that the relatively dry air of the tropical lower stratosphere is being transported poleward more effectively in the MLS versus the

LIMS H_2O cross sections. Note that it is presumed that the patterns of the respective, zonal-mean LIMS and MLS H_2O distributions are correct. Such differences may be an important tracer diagnostic for a climatological change in the meridional transport of the lower stratosphere (Li et al., 2008; Thompson and Solomon, 2009; Tuck et al., 1997). For instance, an increase in the eddy heat flux due to wave activity will accelerate the Brewer-Dobson (BD) circulation and lead to lower zonal mean cold-point temperatures at the tropical tropopause. More specifically, Dhomse et al. (2008) reported on a distinct anti-correlation between tropical water vapor values from 16 to 20 km and the September to February eddy heat flux at 50 hPa of both hemispheres. They showed that the tropical temperature anomalies were cold and the eddy heat flux was enhanced during the period of the MLS measurements. On the other hand, the tropical temperature anomalies are warm during the time of LIMS, indicating a corresponding reduction in the eddy heat flux and the associated BD circulation.

Differences near 60S in the MLS and LIMS H_2O of Figure 2 for the lower stratosphere indicate the effects of enhanced dehydration toward the outer regions of the southern polar vortex in the decades since the Nimbus 7 LIMS experiment. A more complete examination of the state of the southern hemisphere polar winter stratosphere of 1978 should be undertaken to estimate the effects of dehydration at that time and for comparison with the measured values from LIMS in November and late October 1978.

The sequence of MLS water vapor of February, May, and then November (Figures 5b, 6b, and 2b) indicates an annual cycle in H_2O in the lower tropical stratosphere, the so-

called “tape recorder” response first described by Mote et al. (1996). In other words, the location and movement of the MLS hygropause is in good accord with an annual cycle for H_2O, which has its minimum at the cold tropopause in February and is then carried upward slowly through the rest of the year. Figure 7a shows the 7-month time series of tropical (10S to 10N) H_2O from 50 to 10 hPa from LIMS V6. Note that we have plotted time series of the mixing ratio rather than the mixing ratio anomalies because we do not have one complete year of data for defining its annual average. A “tape recorder” signal is clearly evident above the 30-hPa level in Figure 7a. Minimum values occur in February, when the associated LIMS time series of the zonal average T(p) indicate the coldest values (see Figure 7b). The upward extension of low water vapor mixing ratios to above 30 hPa in February may be a consequence of a slight warm bias for the time when the retrieved tropical temperatures are coldest.

Visual inspections of the LIMS water vapor values in the middle stratosphere for November, February, and May (Figures 2, 5, and 6) indicate slightly larger values at middle latitudes in the northern than in the southern hemisphere. In other words, there is a slight hemispheric asymmetry in the H_2O values, most likely due to larger descent rates for polar air from the upper to the middle stratosphere in the northern hemisphere followed by meridional mixing from polar to middle latitudes. There may also be a northern subtropical contributions from the relatively large “entry-level H_2O” (or H_2O_e) associated with the summer monsoon circulation (Jackson et al., 1998). It is less likely that there is a mid-stratosphere influence in the southern hemisphere due to the wintertime polar dehydration over Antarctica (Mote, 1995).

Earlier estimates of H_2O_e from LIMS by Jones et al. (1986) and Hansen and Robinson (1989) must be revised upward now because of the greater values of the V6 H_2O. For example, using the descending LIMS V6 H_2O and the SAMS CH_4 for the months of January through May 1979, we obtain a value of 6.8±0.3 ppmv for the quantity $2CH_4 + H_2O$ at 40 N and between 3 and 10 hPa. Because CH_4 at the tropical tropopause at that time was about 1.5 ppmv, we infer H_2O_e of 3.8±0.3 ppmv. Mid to upper stratosphere values of $2CH_4 + H_2O$ at 40S are only about 6.5 ppmv, so H_2O_e is about 0.3 ppmv less or 3.5 ppmv. This range of H_2O_e values agrees well with that inferred from the in situ and satellite measurements of the late 1980s and the 1990s (see Table 2.4 of Kley et al. (2000)). It is also qualitatively consistent with the warm anomalies of the cold-point tropopause temperatures of the late 1970s.

Both the vertical and along-orbit sampling of the LIMS H_2O dataset represent significant improvements from the V6 profiles. For this reason daily water vapor fields on pressure surfaces exhibit good continuity, making it possible to resolve some of the details of the variations and the large-scale transport of water vapor with altitude, latitude, and longitude. As an example, Figure 8a shows the distribution of LIMS H_2O of 7 February 1979 on the 31.6-hPa surface for the northern hemisphere, as generated from zonal Fourier analyses of the V6 profiles plus minor interpolations for their coefficients in time and onto grid spaces. One can see a region of low H_2O (4.5 ppmv) at about the Greenwich meridian and 55 N latitude; it is co-located with temperatures near 195 K or just above the threshold for deposition to water ice. The associated plot of the LIMS

geopotential height is in Figure 8b. It shows the effects of underlying domes of high pressure over Siberia and the Aleutians, flanking an intense polar vortex region that is being drawn out toward lower latitudes. Qualitatively, there is a large-scale, counterclockwise circulation about the outer edge of the vortex that may have transported lower values of water vapor toward the vortex from middle latitudes, while peeling higher values of H_2O from the vortex edge toward the middle latitudes. A more complete analysis of the transport of H_2O is possible during this period using sequences of daily plots of the water vapor along with calculated wind fields from the concurrent surface maps of the LIMS geopotential heights.

The LIMS instrument and measurement concept is also the prototype for the Sounding of the Atmosphere using Broadband Emission Radiometry (SABER) satellite experiment (Russell et al., 1999), which began measurements in January 2002 and is still operating in 2009. SABER measures water vapor radiance profiles from the tropopause (or cloud tops) to the upper mesosphere and with nearly a 2 km vertical resolution. Its algorithm for obtaining useful water vapor profiles is fashioned after that of LIMS V6, but with the important addition of a forward model for the non-LTE radiances of the mesosphere and its consequences for the retrieval of H_2O profiles down into the upper stratosphere.

The SABER v1.07 algorithm gives water vapor values in the mesosphere that are too large because of small but significant cold biases in the SABER T(p) (Remsberg et al., 2008). The estimates of LIMS V6 accuracy in Table 1 clearly show that small biases in the temperature profile affect the LTE retrieval of water vapor from limb radiances in the

6.4 to 7.3 µm spectral region. However, based on the good agreement between the LIMS V6 and the MLS water vapor distributions, there is every reason to expect that the SABER H_2O profiles will also be of very good quality once the bias in the SABER T(p) is accounted for. Multi-year, near global-scale studies of the transport of middle atmospheric water vapor are anticipated from the LIMS, MLS, and SABER datasets.

6. Conclusions

The radiances of the Nimbus 7 LIMS experiment were reconditioned and new retrievals of them were conducted with a V6 algorithm to make its products more compatible with those of follow-on satellite experiments. Single profiles of the LIMS V6 H_2O have improved precision (5%) and accuracies (19% at 3 hPa, 14% at 10 hPa, and 26% at 50 hPa), as compared with the original V5 product. Qualitative comparisons with the Aura MLS V2.2 H_2O reveal similar patterns and absolute values between about 70 hPa and 3 hPa. However, one should be cautious about interpreting features in the LIMS V6 profiles of the lowermost stratosphere, in particular within about 2 km of the tropopause where the effects of residual emissions from cloud tops may still be present. The profile segments from about 3.0 hPa to 1.3 hPa contain day/night differences of order 0.6 ppmv (or ~10%), due to not having corrected for the effects of non-LTE emissions near to and above the stratopause.

The V6 Level 2 (profile) data can be obtained by ftp download from the Goddard Earth Sciences and Data Information Services Center (http://daac.gsfc.nasa.gov/) under the

menu entitled “Remote Sensing Data”. Individual LIMS V6 profiles have a point spacing of 0.375 km. Their effective vertical resolution is 3.7 km, primarily because of the finite FOV of the LIMS H_2O channel. Retrievals were conducted for every adjacent pair of profiles along the orbits, yielding an effective spacing of one profile for every 1.6 degrees of latitude.

The good precision of the V6 profiles provides for daily surface maps of stratospheric water vapor for studies of its large-scale transport. Although accuracies for single profiles of the LIMS V6 H_2O may be no better than about 15%, the relative accuracies for its zonal mean distributions are much better than that. Analyses of H_2O time series reveal a tropical tape recorder signal plus the effects of a relatively weak, Brewer-Dobson circulation. Average “entry-level” values for the LIMS V6 H_2O vary from 3.5 ppmv as inferred from the data of the southern hemisphere versus 3.8 ppmv from the northern hemisphere.

Acknowledgements. We recognize John Gille and James Russell III (Co-PIs of the LIMS experiment) and the members of the original LIMS Project and Science Teams. The research leading to the improvement and generation of the LIMS V6 Level 2 water vapor dataset was conducted with funds from several NASA NRA proposals and with the consistent support of Jack Kaye of NASA Headquarters. The analyses in this manuscript were conducted with funds from the NASA NRA NNH08ZDA001N for the MAP Program administered by David Considine.

References

Andrews, D. G., Holton, J. R., and Leovy, C. B., Middle Atmosphere Dynamics, Academic Press, New York, 489 pp., 1987.

Butchart, N. and Remsberg, E. E., The area of the stratospheric polar vortex as a diagnostic for tracer transport on an isentropic surface, J. Atmos. Sci., 43, 1319-1339, 1986.

Chiou, E., Remsberg, E. E., Rodgers, C. D., Munro, R., Bevilacqua, R. M., McCormick, M. P., and Russell III, J. M., Proposed reference model for middle atmosphere water vapor, Adv. Space Res., 18, no. 9/10, 59-89, 1996.

Chiou, E. W., McCormick, M. P., McMaster, L. R., Chu, W. P., Larsen, J. C., Rind, D., and Oltmans, S., Intercomparison of stratospheric water vapor observed by satellite experiments: stratospheric aerosol and gas experiment II versus limb infrared monitor of the stratosphere and atmospheric trace molecule spectroscopy, J. Geophys. Res., 98, 4875-4887, 1993.

Dhomse, S., Weber, M., and Burrows, J., The relationship between tropospheric wave forcing and tropical lower stratospheric water vapor, Atmos. Chem. Phys., 8, 471-480, 2008.

Fueglistaler, S. and Haynes, P. H., Control of interannual and longer-term variability of stratospheric water vapor, J. Geophys. Res., 110, D24108, doi:10.1029/2005JD006019, 2005.

Garcia, R. and Solomon, S., A new numerical model of the middle atmosphere, 2. Ozone and related species, J. Geophys. Res., 99, 12,937-12,951, 1994.

Gille, J. C. and Russell III, J. M., The limb infrared monitor of the stratosphere: experiment description, performance, and results, J. Geophys. Res., 89, 5125-5140, 1984.

Gille, J. C., Lyjak, L. V., and Smith, A. K., The global residual mean circulation in the middle atmosphere for the northern winter period, J. Atmos. Sci., 44, 1437-1452, 1987.

Gray, L. J. and Pyle, J. A., The semiannual oscillation and equatorial tracer distributions, Q. J. R. Meteorol. Soc., 112, 387-407, 1986.

Hansen, A. R. and Robinson, G. D., Water vapor and methane in the upper stratosphere: an examination of some of the Nimbus 7 measurements, J. Geophys. Res., 94, 8474-8484, 1989.

Jackson, D. R., Driscoll, S. J., Highwood, E. J., Harries, J. E., and Russell III, J. M., Troposphere to stratosphere transport at low latitudes as studies using HALOE

observations of water vapour 1992-1997, Quart. J. Roy. Meteorol. Soc., 124, 169-192, 1998.

Jones, R. L. and Pyle, J. A., Observations of CH_4 and N_2O by the NIMBUS 7 SAMS: a comparison with in situ data and two-dimensional numerical model calculations, J. Geophys. Res., 89, 5263-5279, 1984.

Jones, R. L., Pyle, J. A., Harries, J. E., Zavody, A. M., Russell III, J. M., and Gille, J. C., The water vapor budget of the stratosphere studied using LIMS and SAMS satellite data, Q. J. R. Meteorol. Soc., 112, 1127-1143, 1986.

Kerridge, B. J. and Remsberg, E. E., Evidence from the limb infrared monitor of the stratosphere for nonlocal thermodynamic equilibrium in the nu2 mode of mesospheric water vapour and the nu3 mode of stratospheric nitrogen dioxide, J. Geophys. Res., 94, 16,323-16,342, 1989.

Kley, D., Russell III, J. M., and Phillips, C., Eds., SPARC Assessment of Upper Tropospheric and Stratospheric Water Vapour, World Climate Research Program (WCRP) Report No. 113, World Meteorological Organization (WMO) Technical Document 1043, 312 pp., 2000.

Lambert, A., Read, W. G., Livesey, N. J., Santee, M. L., Manney, G. L., Froidevaux, L., Wu, D. L., Schwartz, M. J., Pumphrey, H. C., Jimenez, C., Nedoluha, G. E., Cofield, R.

E., Cuddy, D. T., Daffer, W. H., Drouin, B. J., Fuller, R. A., Jarnot, R. F., Knosp, B. W., Pickett, H. M., Perun, V. S., Snyder, W. V., Stek, P. C., Thurstans, R. P., P. A. Wagner, Waters, J. W., Jucks, K. W., Toon, G. C., Stachnik, R. A., Bernath, P. F., Boone, C. D., Walker, K. A., Urban, J., Murtagh, D., Elkins, J. W., and Atlas, E., Validation of the Aura Microwave Limb Sounder middle atmosphere water vapor and nitrous oxide measurements, J. Geophys. Res., 112, D24S36, doi:10.1029/2007JD008724, 2007.

LeTexier, L., Solomon, S., and Garcia, R. R., The role of molecular hydrogen and methane oxidation in the water vapour budget of the stratosphere, Q. J. R. Meteorol. Soc., 114, 281-296, 1998.

Li, F., Austin, J., and Wilson, J., The strength of the Brewer-Dobson circulation in a changing climate: coupled chemistry-climate model simulations, J. Climate, 21, 40-57, 2008.

Mertens, C. J.,Mlynczak, M. J., Lopez-Puertas, M., and Remsberg, E. E., Impact of non-LTE processes on middle atmospheric water vapor retrievals from simulated measurements of 6.8 micrometer Earth limb emission, Geophys. Res. Lett., vol. 29, no. 9, pp. 2-1 to 2-4, 2002.

Mote, P. W., Reconsideration of the cause of dry air in the southern middle latitude stratosphere, Geophys. Res. Lett., 22, 2025-2028, 1995.

Mote, P. W., Rosenlof, K. H., Holton, J. R., Harwood, R. S., and Waters, J. W., An atmospheric tape recorder: the imprint of tropical tropopause temperatures on stratospheric water vapor, J. Geophys. Res., 102, 3989-4006, 1996.

Remsberg, E. E. and Russell III, J. M., The near global distributions of middle atmospheric H_2O and NO_2 measured by the Nimbus 7 LIMS experiment, in Transport Processes in the Middle Atmosphere, edited by G. Visconti and R. Garcia, Reidel, 87-102, 1987.

Remsberg, E. E., Russell III, J. M., and Wu, C.-Y., An interim reference model for the variability of the middle atmosphere water vapor distribution, Adv. Space Res., 10, no. 6, 51-64, 1990.

Remsberg, E. E., Russell III, J. M., Gordley, L. L., Gille, J. C., and Bailey, P. L., Implications of the stratospheric water vapor distribution as determined from the NIMBUS 7 LIMS experiment, J. Atmos. Sci., 41, 2934-2945, 1984a.

Remsberg, E. E., Russell III, J. M., Gille, J. C., Gordley, L. L., Bailey, P. L., Planet, W. G., and Harries, J. E., The validation of NIMBUS 7 measurements of ozone, J. Geophys. Res., 89, 5161-5178, 1984b.

Remsberg, E. E., Kurzeja, R. J., Haggard, K. V., Russell III, J. M., and Gordley, L. L., Description of data on the Nimbus 7 LIMS Map Archive Tape—Ozone and Nitric Acid, NASA Tech. Paper No. 2625, available from NTIS, Springfield, VA, 71 pp., 1986.

Remsberg, E. E., Gordley, L. L., Marshall, B. T., Thompson, R. E., Burton, J., Bhatt, P., Harvey, V. L., Lingenfelser, G. S., and Natarajan, M., The Nimbus 7 LIMS Version 6 radiance conditioning and temperature retrieval methods and results, J. Quant. Spectrosc. Rad. Transf., 86, 395-424, doi:10.1016/j.jqsrt.2003.12.007, 2004.

Remsberg, E., Lingenfelser, G., Natarajan, M., Gordley, L., Marshall, B. T., and Thompson, E., On the quality of the Nimbus 7 LIMS version 6 ozone for studies of the middle atmosphere, J. Quant. Spectrosc. Rad. Transf., 105, 492-518, doi:10.1016/j.jqsrt.2006.12.005, 2007

Remsberg, E. E., Marshall, B. T., Garcia-Comas, M., Krueger, D., Lingenfelser, G. S., Martin-Torres, J., Mlynczak, M. G., Russell III, J. M., Smith, A. K., Zhao, Y., Brown, C., Gordley, L. L., Lopez-Gonzalez, M. J., Lopez-Puertas, M., She, C.-Y., Taylor, M. J., and Thompson, R. E., Assessment of the quality of the Version 1.07 temperature-versus-pressure profiles of the middle atmosphere from TIMED/SABER, J. Geophys. Res., 113, D17101, doi:10.1029/2008JD010013, 2008.

Rosenlof, K. H., Oltmans, S. J., Kley, D., Russell III, J. M., Chiou, E.-W., Chu, W. P., Johnson, D. J., Kelly, K. K., Michelsen, H. A., Nedoluha, G. E., Remsberg, E. E., Toon,

G. C., and McCormick, M. P., Stratospheric water vapor increases over the past half century, Geophys. Res. Lett., 28, 1195-1198, 2001.

Rothman, L. S., Rinsland, C. P., Goldman, A., Massie, S. T., Edwards, D. P., Flaud, J.-M., Perrin, A., Camy-Peyret, C., Dana, V., Mandin, J.-Y., Schroeder, J., McCann, A., Gamache, R. R., Wattson, R. B., Yoshino, K., Chance, K. V., Jucks, K. W., Brown, L. R., Nemtchinov, V., and Varanasi, P., The HITRAN molecular spectroscopic database and HAWKS (HITRAN Atmospheric WorKStation): 1996 edition, J. Quant. Spectrosc. & Rad. Transfer, 60, 665-710, 1998.

Russell III, J. M., An interim reference model for the middle atmosphere water vapor distribution, Adv. Space Res., 7, no. 9, 5-15, 1987.

Russell III, J. M., Gille, J. C., Remsberg, E. E., Gordley, L. L., Bailey, P. L., Fischer, H., Girard, A., Drayson, S. R., Evans, W. F. J., and Harries, J. E., Validation of water vapor results measured by the limb infrared monitor of the stratosphere experiment on NIMBUS 7, J. Geophys. Res., 89, 5115-5124, 1984.

Russell III, J. M., Mlynczak, M. G., Gordley, L. L., Tansock, J., and Esplin, R., An overview of the SABER experiment and preliminary calibration results, in Proceedings of the SPIE, 3756, 44th Annual Meeting, Denver, CO, July 18-23, 277-288, 1999.

Thibault, F., Menoux, V., LeDoucen, R., Rosenmann, L., Hartmann, J.-M., and Boulet, C., Infrared collision-induced absorption by O_2 near 6.4 μm for atmospheric applications: measurements and empirical modeling, Appl. Opt., 36, 563-567, 1997.

Thompson, D. W. J. and Solomon, S., Understanding recent stratospheric climate change, J. Climate, 22, 1934-1943, 2009.

Tuck, A. F., Baumgardner, D., Chan, K. R., Dye, J. E., Elkins, J. W., Hovde, S. J., Kelly, K. K., Loewenstein, M., Margitan, J. J., May, R. D., Podolske, J. R., Proffitt, M. H., Rosenlof, K. H., Smith, W. L., Webster, C. R., and Wilson, J. C., The Brewer-Dobson circulation in the light of high altitude in situ aircraft observations, Quart. J. Roy. Meteorol. Soc., 123, 1-69, 1997.

WMO (World Meteorological Organization), Scientific Assessment of Ozone Depletion: 2006, Global Ozone Research and Monitoring Project—Report No. 50, 572 pp., Geneva, Switzerland, 2007.

Figure Legends

1. Locations and relative sizes of the LIMS channel fields-of-view (FOV) projected to the limb at the tops and bottom of a down/up scan pair.

2. (a) Zonal mean of LIMS V6 descending orbital (nighttime) H_2O for 15 November 1978. Contour interval is 1.0 ppmv; (b) Zonal mean of MLS V2.2 H_2O for 15 November 2004.

3. Zonal-mean cross section of the ascending (day) minus descending (night) differences in LIMS V6 H2O for 15 November 1978. Contour interval is 0.2 ppmv.

4. Profiles of the minimum standard deviation (SD) values of LIMS V6 H_2O (in %) from its sets of descending (open diamonds) and ascending (solid diamonds) orbital crossings between 25S and 35S latitude on 1 February 1979.

5. As in Figure 2, but (a) for LIMS V6 descending H_2O of 15 February 1979 and (b) for MLS for 15 February 2005.

6. As in Figure 2, but (a) for LIMS V6 descending H_2O of 16 May 1979 and (b) for MLS for 16 May 2005.

7. (a) Time series of zonally-averaged LIMS V6 H_2O mixing ratio (in ppmv) for 10 S to 10 N and from 50 to 10 hPa; color contour increment is 0.2 ppmv and plot extends only to 25 May 1979. (b) As in 7(a), but for LIMS V6 temperatures with a color change every 4 K. Tic marks on the abscissa denote Day 15 of each month.

8. Polar plot of LIMS V6 northern hemisphere data at 31.6 hPa (mb) for 7 February 1979--(a) H_2O with a contour interval of 0.5 ppmv; (b) geopotential height from 21.2 to 23.6 with a contour interval of 0.1 gpkm.

Table 1—Estimates of Precision and Accuracy (in %) for Profiles of LIMS V6 H_2O

Pressure (hPa)	*100*	*50*	*30*	*10*	*5*	**3**
Random (or PRECISION)	5	5	5	5	6	9
Radiometric Bias	5	5	5	5	5	5
Temperature Bias (Amt. of T Bias)	16 (1.1 K)	18 (1.3 K)	11 (1.1 K)	8 (1.0 K)	14 (1.5 K)	15 (1.6 K)
H_2O Line Parameters (8%)	8	8	8	8	8	8
O_2 Cross Section (10%)	11	6	2	1	0	0
Forward Model	5	5	5	5	5	5
Main IFOV Lobe	15	15	5	5	5	5
RSS of Bias Errors (or ACCURACY)	27	26	16	14	18	19

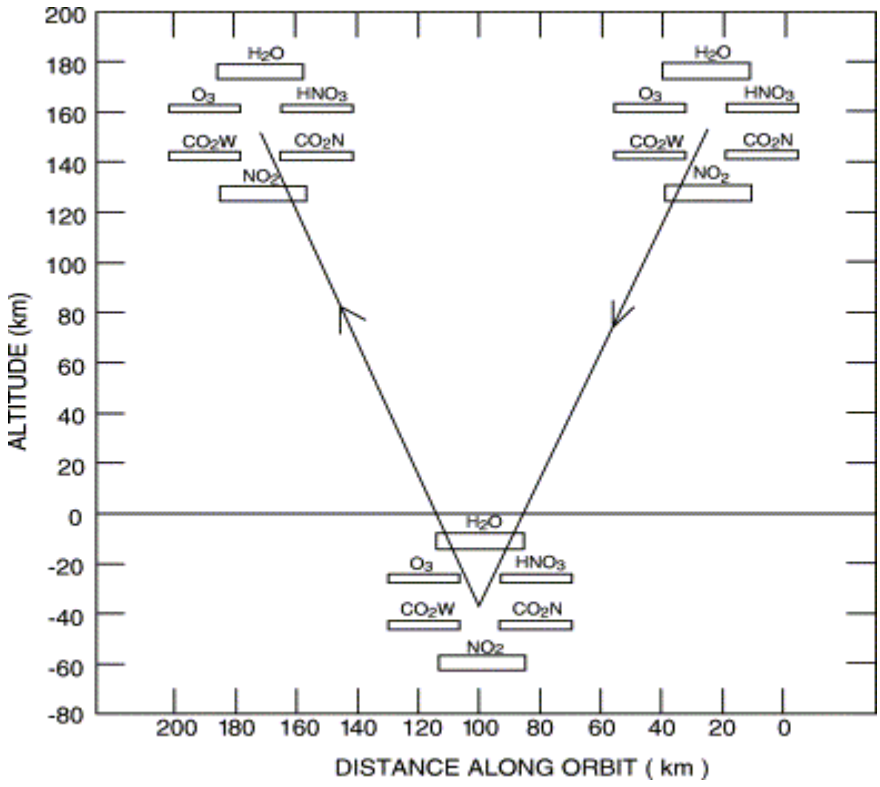

Figure 1—Locations and relative sizes of the LIMS channel fields-of-view (FOV) projected to the limb at the tops and bottom of a down/up scan pair.

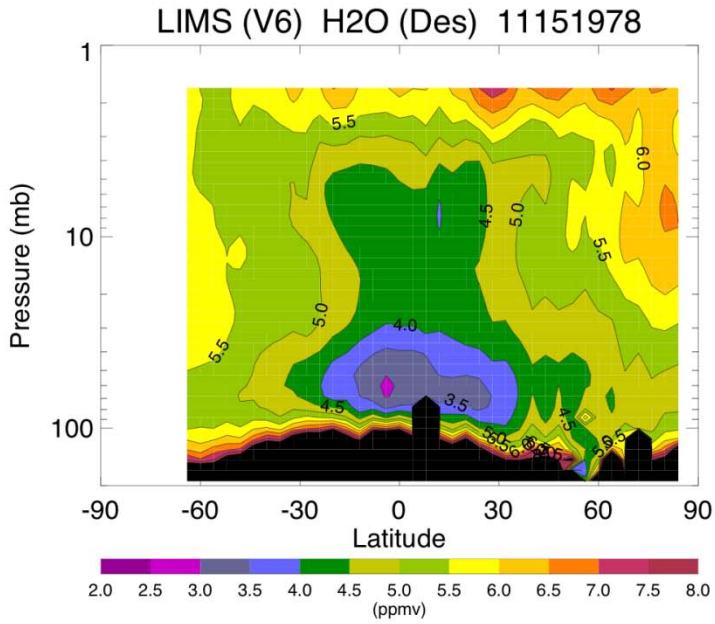

Figure 2a—Zonal mean of LIMS V6 descending orbital (nighttime) H2O for 15 November 1978. Contour interval is 1.0 ppmv.

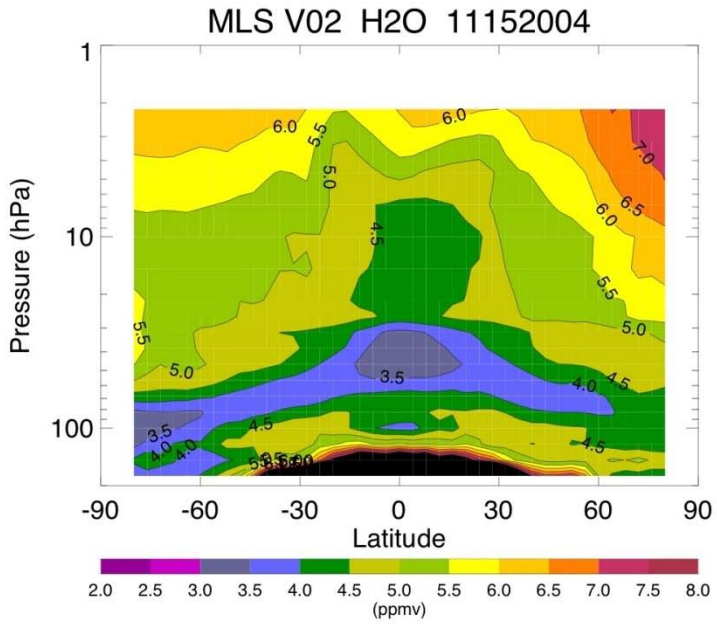

Figure 2b—Zonal mean of MLS V2.2 H2O for 15 November 2004.

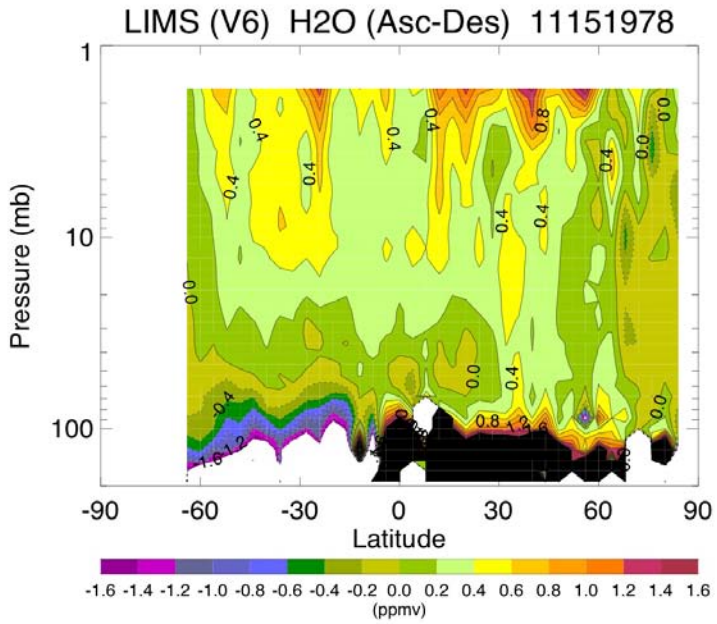

Figure 3—Zonal-mean cross section of the ascending (day) minus descending (night) differences in LIMS V6 H2O for 15 November 1978. Contour interval is 0.2 ppmv.

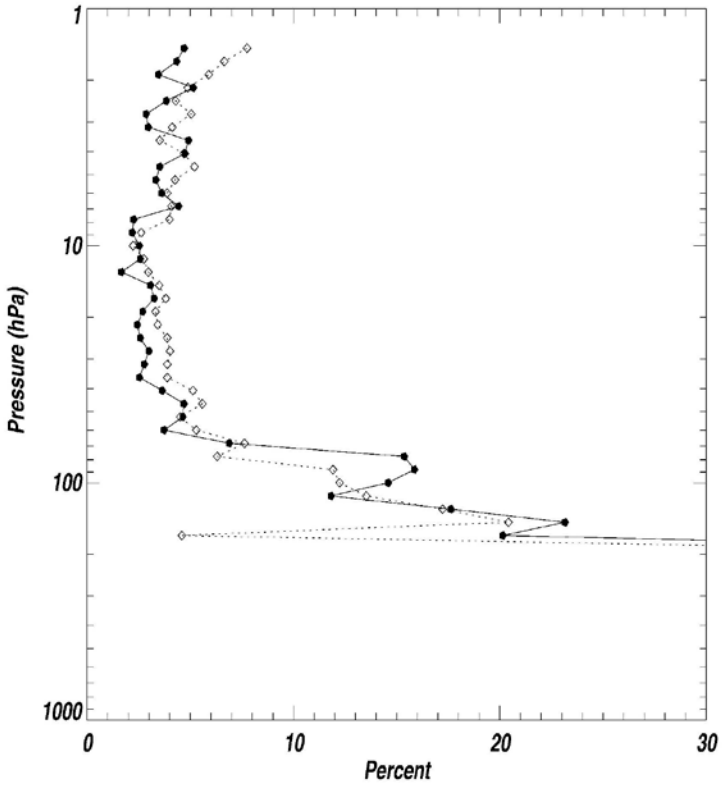

Figure 4—Profiles of the minimum standard deviation (SD) values of LIMS V6 H2O (in %) from its sets of descending (open diamonds) and ascending (solid diamonds) orbital crossings between 25S and 35S latitude on 1 February 1979.

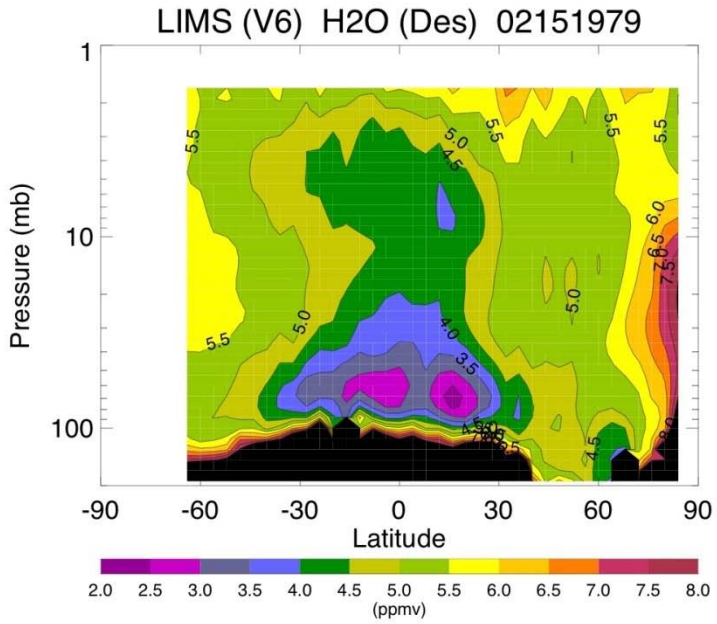

Figure 5a—As in Figure 2, but for LIMS V6 descending H_2O of 15 February 1979.

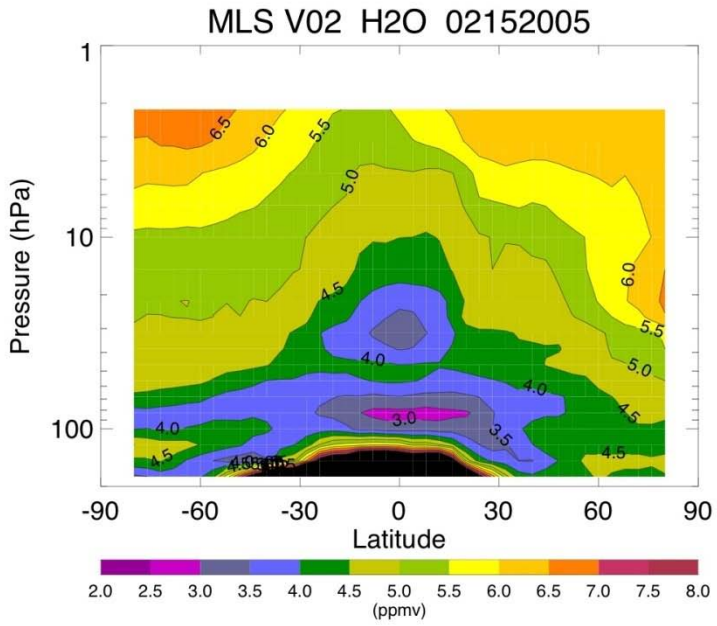

Figure 5b—As in Figure 2, but for MLS for 15 February 2005.

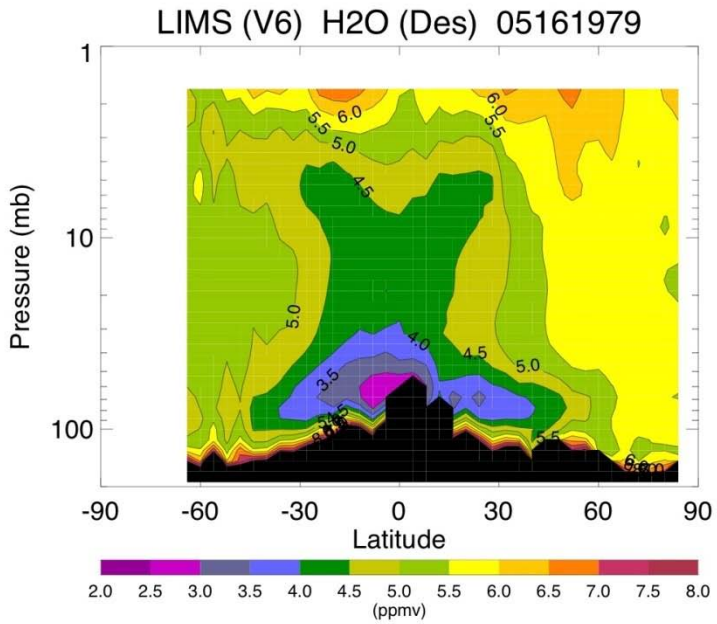

Figure 6a—As in Figure 2, but for LIMS V6 descending H_2O of 16 May 1979.

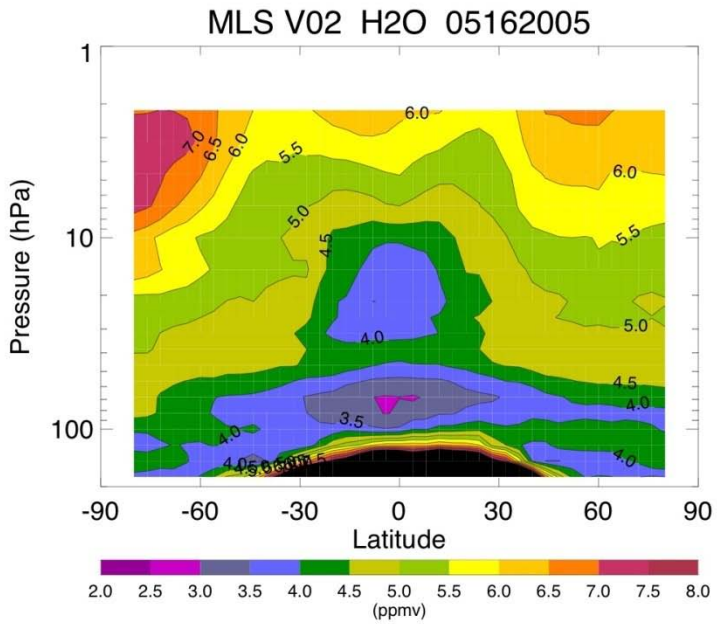

Figure 6b—As in Figure 2, but for MLS for 16 May 2005.

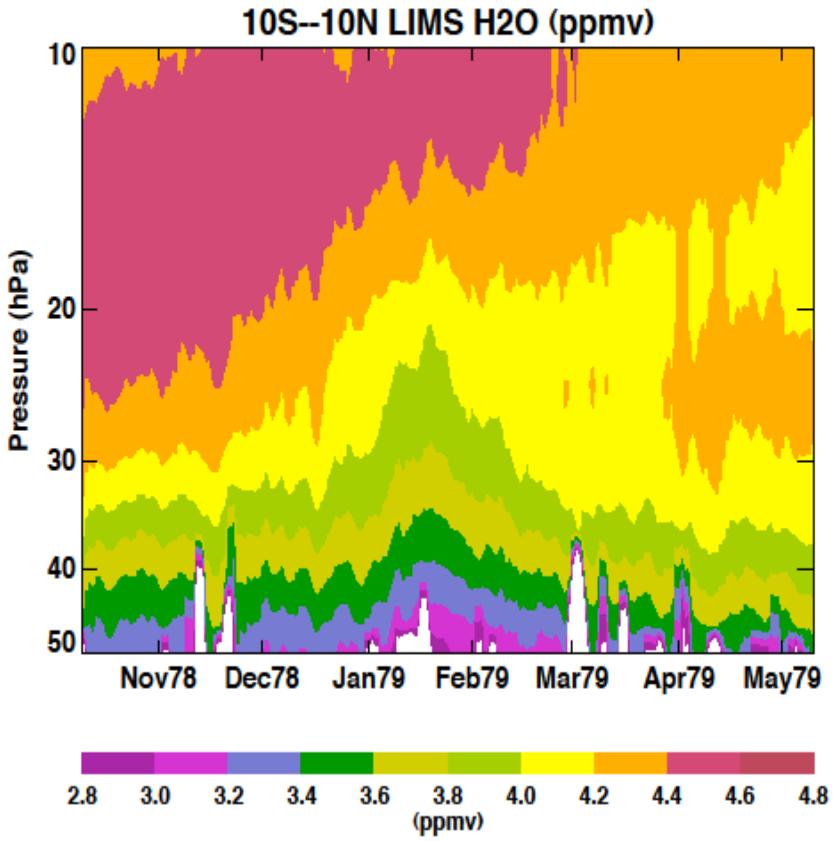

Figure 7a— Time series of zonally-averaged LIMS V6 H_2O mixing ratio (in ppmv) for 10 S to 10 N and from 50 to 10 hPa; color contour increment is 0.2 ppmv and plot extends only to 25 May 1979.

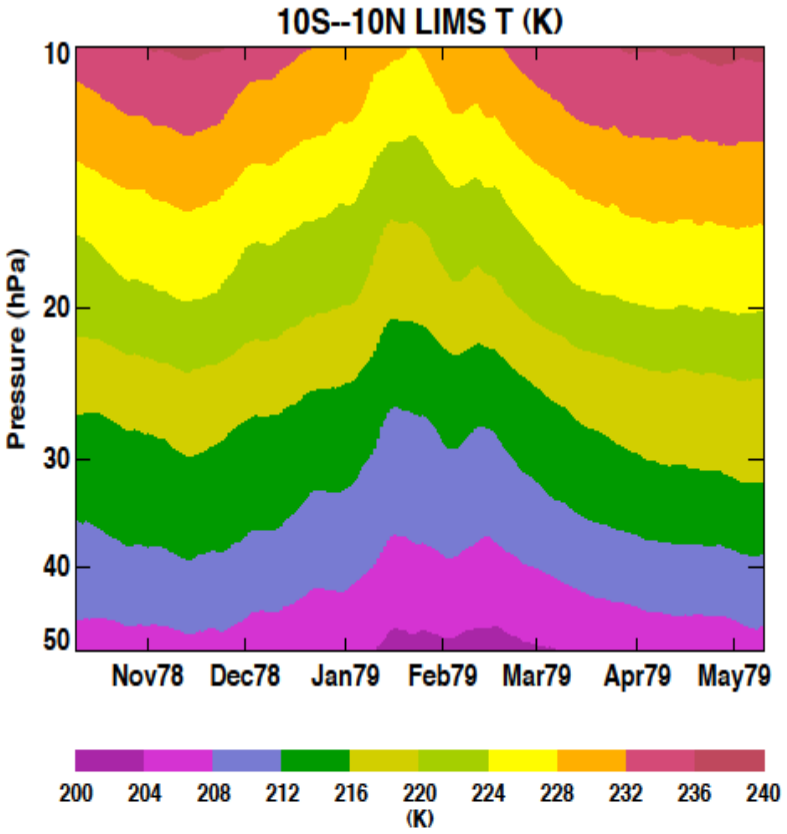

Figure 7b--As in 7(a), but for LIMS V6 temperatures with a color change every 4 K. Tic marks on the abscissa denote Day 15 of each month.

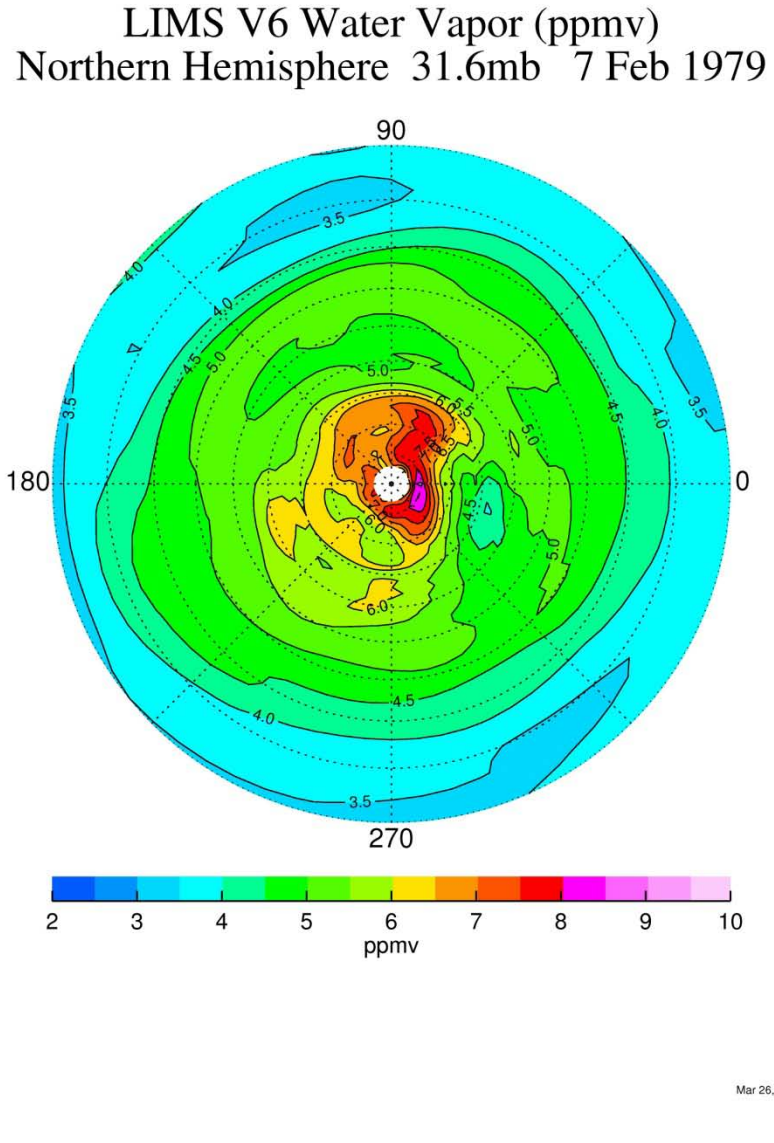

Figure 8a—Polar plot of LIMS V6 northern hemisphere data at 31.6 hPa (mb) for 7 February 1979—H2O with a contour interval of 0.5 ppmv.

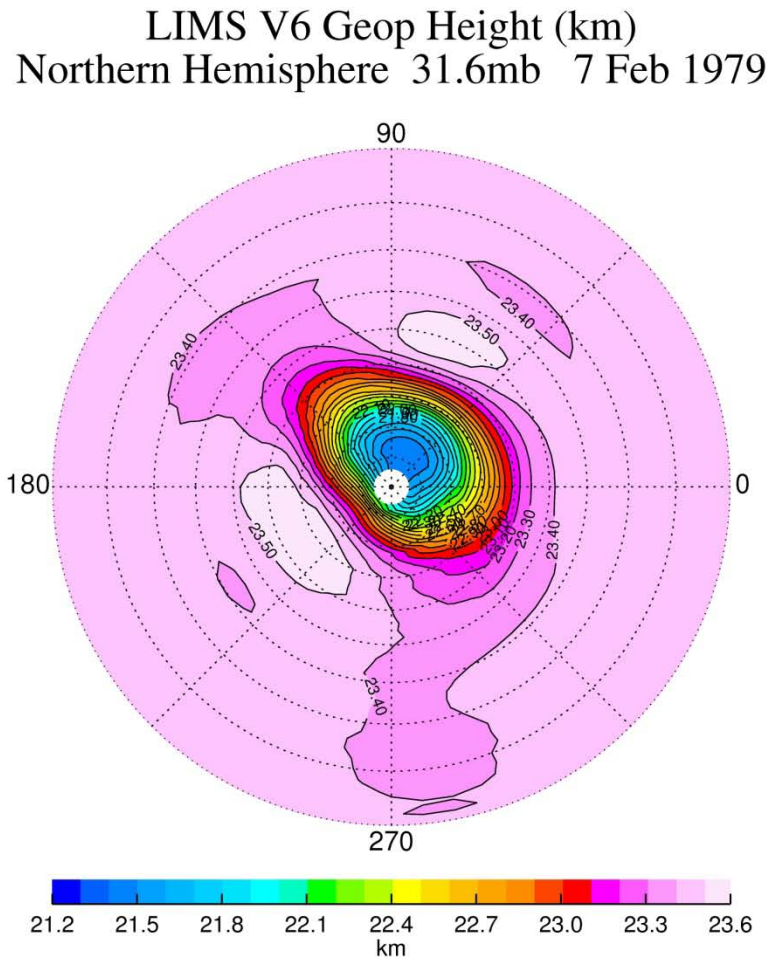

Figure 8b—Polar plot of LIMS V6 northern hemisphere data at 31.6 hPa (mb) for 7 February 1979—geopotential height from 21.2 to 23.6 with a contour interval of 0.1 gpkm.